6560 J. Med. Chem. 2010, 53, 6560–6571
DOI: 10.1021/jm100398z

Journal of Medicinal Chemistry Article

Synthesis, Anti-Inflammatory Activity, and in Vitro Antitumor Effect of a Novel Class of Cyclooxygenase Inhibitors: 4-(Aryloyl)phenyl Methyl Sulfones

Youssef Harrak,[†] Giovanni Casula,[§] Joan Basset,[†] Glòria Rosell,[†] Salvatore Plescia,[§] Demetrio Raffa,[§] Maria Grazia Cusimano,[§] Ramon Pouplana,*[,‡] and Maria Dolors Pujol*[,†]

[†]*Laboratori de Química Farmacèutica* (*Unitat Associada al CSIC*), *and* [‡]*Laboratori de Físico-Química, Facultat de Farmàcia, Universitat de Barcelona, Av. Diagonal 643, E-08028 Barcelona, Spain, and* [§]*Dipartamento di Chimica e Tecnologie Farmaceutiche, Facoltà di Farmacia, Università degli Studi di Palermo, Via Archirafi, 32-90123 Palermo, Italy*

Received March 30, 2010

Following our previous research on anti-inflammatory drugs (NSAIDs), we report on the design and synthesis of 4-(aryloyl)phenyl methyl sulfones. These substances were characterized for their capacity to inhibit cyclooxygenase (COX-1 and COX-2) isoenzymes. Molecular modeling studies showed that the methylsulfone group of these compounds was inserted deep in the pocket of the human COX-2 binding site, in an orientation that precludes hydrogen bonding with Arg120, Ser353, and Tyr355 through their oxygen atoms. The *N*-arylindole **33** was the most potent inhibitor of COX-2 and also the most selective (COX-1/COX-2 IC_{50} ratio was 262). The indole derivative **33** was further tested in vivo for its anti-inflammatory activity in rats. This compound showed greater inhibitory activity than ibuprofen. Other compounds (**20**, **26**, **9**, and **30**) showed strong activity against carrageenan-induced inflammation. The latter compounds showed a weak capacity to inhibit the proliferation of human cell lines K562, NCI-H460, and HT-29 in vitro.

Introduction

Nonsteroidal anti-inflammatory drugs (NSAIDs[a]) are widely used to alleviate inflammation and pains associated with many pathological conditions and are often the initial therapy for common inflammation. NSAIDs inhibit the biosynthesis of prostaglandins (PGs). In general, biosynthesis involves the conversion of arachidonic acid to prostaglandin G_2 (PGH_2), a reaction catalyzed by the sequential action of cyclooxygenase (COX). Most NSAIDs inhibit COX-1 and COX-2 isoforms.[1−3] COX-1 is responsible for the synthesis of cytoprotective prostaglandins in the gastrointestinal tract and for the proaggregatory thromboxane in blood platelets.[4] COX inhibitors have recently been reported to have a protective effect against colon cancer and Alzheimer's disease. Moreover, these compounds continue to be the most commonly used remedies for rheumatic diseases.[5] Several studies have indicated that the COX inhibitors may prevent colon cancer.[6] The molecular mechanism responsible for the chemopreventive action of NSAIDs is not understood. However, recent literature has revealed several mechanisms involved in the inhibition of proliferation or invasive growth, such as apoptosis,[7] angiogenesis,[8] and activation of protein kinase G.[9] NSAIDs are potent antioxidants that exert both anti-inflammatory and antitumor activity. In this regard, ibuprofen inhibits tumor growth and liver metastasis. While regular treatment with NSAIDs correlates with a reduced risk of lymphoma and leukemia development, long-term use of acetaminophen enhances the development of leukemia.[10] Of 20 published epidemiologic studies focusing on the association between NSAIDs and the risk of cancer in humans, 13 reported a significant reduction of the disease.[10] Although epidemiological studies have demonstrated that NSAID compounds are effective in chemoprevention and may also provide a treatment for several cancers, more detailed studies are required before their medicinal application.[11] Thus, ibuprofen inhibits cell proliferation in vitro in human cell lines (HT-29) and also potentiates the antitumor activity of agents such as 5-fluorouracile.[12] Sulindac and celecoxib inhibit the growth of adenomatous polyps of patients with familial adenomatous polyposis.[13] The development of safe and effective pharmaceutical compounds is complicated. However, recent studies suggest that the long-term use of selective COX-2 inhibitors is limited because of cardiovascular thrombotic events related to the aggregatory properties of these drugs.[14] Moreover, COX-2 makes a significant contribution to the production of inflammatory PGs, and the inhibition of COX-2 attenuates the expression of inflammatory mediators such as TNF-α, iNOS, and IL-1β.[15]

In an attempt to rationalize the selective activity of COX-1/COX-2 and the cytotoxicity of NSAIDs, here we designed a series of new compounds from classic arylpropionic acids, such as ketoprofen and suprofen (Figure 1), which are considered nonselective for COX-1 and COX-2. The diarylketone subunit was slightly modified, and the propionic acid group was changed to methylsulfone, a more lipophilic group with acidic properties. The modifications were chosen to evaluate whether the haptophore moiety of arylpropionic acids

*To whom correspondence should be addressed. For M.D.P.: phone, +34-93-4024534; fax, +34-93-4035941; e-mail, mdpujol@ub.edu. For R.P.: phone, +34-93-4024557; fax, +34-93-40325987; e-mail, rpouplana@ub.edu.

[a] Abbreviations: COX-1, cyclooxigenase-1; COX-2; cyclooxigenase-2; NSAIDs, nonsteroidal anti-inflammatory drugs; PG, prostaglandin; PGH_2, prostaglandin G_2; MTT, 3(4,5-dimethylthiazol-2-yl)-2,5-diphenyltetrazolium bromide; SAR, structure−activity relationship; QSAR, quantitative structure−activity relationship.

 Published on Web 08/30/2010

influenced the selectivity of COX isoforms for methylsulfones. Here we report on the synthesis of a new series of sulfones as a novel class of NSAIDs and also their anti-inflammatory and antitumor activity and structure−activity relationships.

Chemical Section

The methods used for the synthesis of arylsulfones are convenient because the reagents are readily available and the protocols straightforward.

The general synthetic routes are illustrated in Schemes 1−5. These methylsulfones were prepared by oxidation of the 2- or 3-(*p*-(methylthio)benzoyl) heterocycle to the corresponding sulfone using *m*-CPBA (Scheme 1). The intermediate diarylketone (**3**−**8** and **16**−**19**) was obtained in a two steps from the corresponding arylaldehyde and *p*-bromothioanisole using butyllithium for the Br/Li interchange,[16] followed by oxidation of the carbinol obtained (**2a**−**f**) (Scheme 1) or directly by acylation of the thioanisole **15** with the corresponding arylacyl chloride under classical conditions (Scheme 2).[17]

The arylketones (**16**−**19**) were transformed to the corresponding methylsulfones **20**−**23** by oxidation with *m*-CPBA (Scheme 2).[18]

The 2-arylpyridine **26** was prepared by a coupling reaction of 2-bromopyridine (**24**) and the *p*-methylthiobromobenzene (**1**) under classical Ullmann conditions[19] followed by oxidation of the methylthio group using *m*-CPBA (Scheme 3). The method using *m*-CPBA was highly effective and simple for the oxidation to methylsulfones.

The *N*-(2-fluorophenyl)pyrrole **27** was obtained from 2-fluoroaniline following the Paal−Knorr condensation.[20] The racemic methylsulfone **29** was prepared by intramolecular cyclization of the racemic carbinol **2d** in basic media followed by oxidation of the methylthio intermediate **28** as a racemate with *m*-CPBA in the optimized conditions described above (Scheme 4). Enantiomers of **29** were not separated, and the biological tests were performed with the racemic mixture.

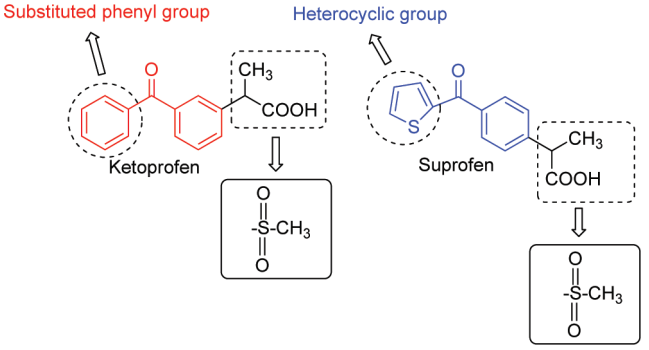

Figure 1. Structure of NSAIDs.

We developed a synthetic approach for *N*-arylamines **30**−**33** using Pd catalysts for the amination of aryl halides (Scheme 5). We previously reported the synthesis of the diarylamine **30**, the *N*-arylpyrrole **32**, and the *N*-arylindole **33**.[21] We included these compounds in this study in order to facilitate structure−activity relation studies.

Biological Results. Discussion

We evaluated the capacity of these compounds to inhibit COX-1 and COX-2 in vitro. The potency and selectivity with respect to two isoforms was determined from IC_{50}values, expressed as the concentration of compound required to inhibit 50% of the initial rate of the amount of PG_s by enzyme immunoassay.

Two compounds (**9** and **13**) were nonselective COX-2 inhibitors (selectivity index SI = 1), whereas seven (**11**, **31**, **29**, **21**, **20**, **32**, and **12**) were moderately selective against this isoform (SI = 2.1, 4.2, 6.7, 9.4, 10, 10.1, 4.2, respectively). In contrast four compounds (**10**, **22**, **30**, and **33**) showed very high COX-2 selectivity indexes (36.6, 150, 70.3, and 262, respectively).

Compounds **14** and **23** showed moderate COX-2 selectivity indexes. The indole derivative **11** had an inhibition profile similar to **13**, whereas the diarylketone **23** showed less inhibition capacity than the bromo analogue **22.**

The compound most selective for COX-2, **33**, was a weak inhibitor of COX-1 (IC_{50} = 78.7 μM) and a potent inhibitor of COX-2 (IC_{50} = 0.3 μM). As a positive control, we used NS398

Scheme 2[a]

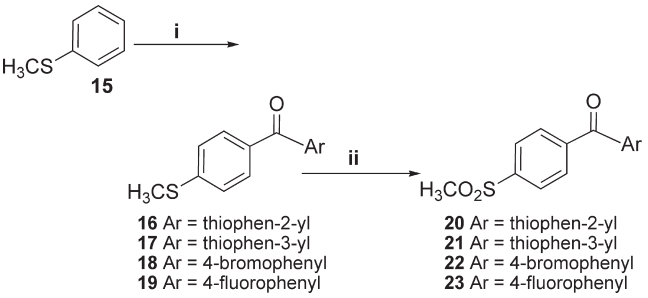

[a] Reaction conditions: (i) $ArCOCl/CH_2Cl_2$; (ii) *m*-CPBA, 0 °C.

Scheme 3[a]

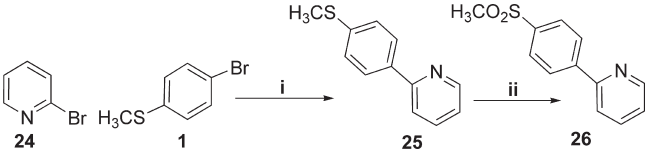

[a] Reaction conditions: (i) Cu/K_2CO_3; (ii) *m*-CPBA, 0 °C.

Scheme 1[a]

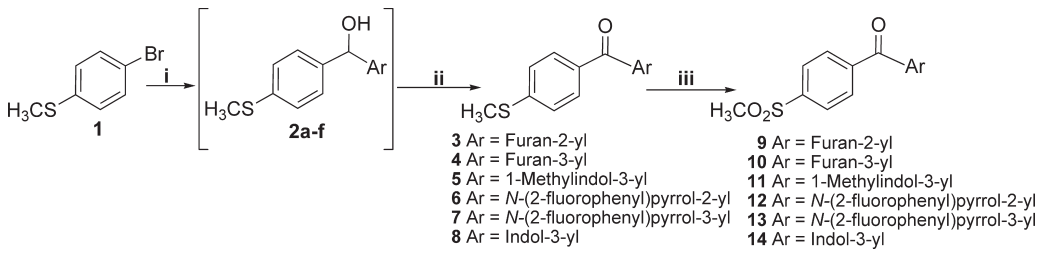

[a] Reaction conditions: (i) BuLi/ArCHO; (ii) MnO_2/CH_2Cl_2, (iii) *m*-CPBA, 0 °C.

Scheme 4[a]

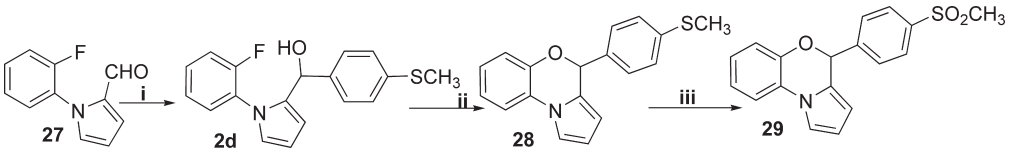

[a] Reaction conditions: (i) **1**, BuLi, THF, −78 °C; (ii) NaH/DMF; (iii) *m*-CPBA, 0 °C.

Scheme 5[a]

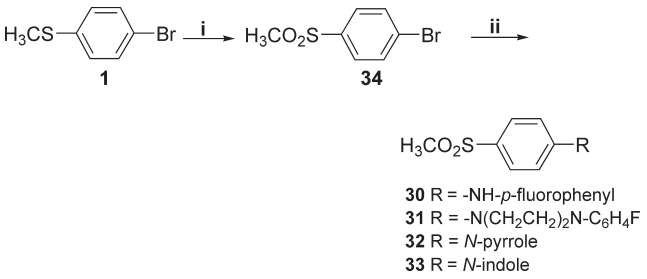

[a] Reaction conditions: (i) *m*-CPBA, 0 °C; (ii) $Pd[P(o\text{-tolyl})_3]_2Cl_2$, BINAP, Cs_2CO_3, NHR^1R^2.

which showed an inhibition of 73.2% for COX-2 and 14.1% for COX-1 when used at a concentration of 0.2 μM (Table 1).

All the compounds tested inhibited COX. Comparison results with standard drugs ibuprofen, NS398, celecoxib, and rofecoxib are listed in Table 1. The *N*-arylindole **33** elicited maximum inhibition of COX-2, whereas ibuprofen showed efficacy in inhibiting both COX-1 and COX-2. Also, the diarylketone **22** exhibited greater activity (1 ± 0.15 μM) than **23** (7.7 ± 0.28 μM), in which the substituent of the aryl was a fluorine instead of a bromine atom. Thus, **33** and **22** showed 262 and 150 times more inhibitory activity against COX-2 than COX-1, respectively. Moreover, the indole derivative **33** presents inhibition of COX-2 equivalent to known AINEs such as celecoxib and rofecoxib while its COX-2/COX-1 selectivity was 4 and 8 times greater, respectively.

In order to test the structural requirements, we studied the isomeric compounds. The inhibitory activity of 3-substituted furan (**10**) against COX-2 was greater than the observed for the 2-substituted furan (**9**). Also, the anti-inflammatory activity of the bioisoster **21**, which had a 3-substituted thiophene, was found to be greater than that of 2-substituted thiophene (**20**). In the pyrrole ring the 3-substituted compound showed 2-fold more COX-2 inhibition than the corresponding 2-substituted isomer (comparison of **13** with **12**). The piperazine **31** caused 9-fold reduction in COX-2 inhibition compared with the diarylamine **30**. In comparison with the indole (**33**), the pyrrole derivative (**32**) reduced 30 times the COX-2 inhibition. The methylation of *N*-indole (compound **14**) caused a decrease in COX-2 inhibition that was 4-fold that produced by compound **11**. These compounds were then assessed for anti-inflammatory activity by using the carrageenan rat paw edema assay.

The characteristic feature of the title compounds is the presence of a sulfone group at the phenyl ring. Compounds were tested two times at 70 mg/kg po, and the results were compared with those registered for standard drugs such as ibuprofen. The thiophene derivative **20** elicited maximum inhibition of edema (59.7% and 56% at 3 and 4 h postadministration, respectively) (Table 2). This compound was the most potent of this series, showing twice more activity than the parent compound ibuprofen. Moreover, **20** exhibited extended action, and 5 h after oral administration (4 h postcarrageenan) this compound was 2.40 times more active than ibuprofen.

Table 1. In Vitro Inhibition of COX-1 and COX-2 by Compounds **9**−**14**, **20**−**23**, **26**, **29**, and **30**−**33**[a]

	% inhibition		
	IC_{50} [μM]		
compd	COX-1	COX-2	selectivity index SI = COX-1/COX-2
9	15.1 ± 0.94	19.2 ± 1.80	0.79
10	150 ± 11.30	4.1 ± 1.00	36.6
11	76.4 ± 8.50	36.8 ± 6.60	2.1
12	183 ± 15.3	43.3 ± 5.70	4.20
13	34.6 ± 1.65	19.7 ± 2.70	1.76
14	26.7 ± 2.74	9.4 ± 0.36	2.8
20	231.2 ± 3.10	23.1 ± 3.00	10
21	143.7 ± 4.20	15.2 ± 2.10	9.40
22	150.0 ± 4.20	1 ± 0.15	150
23	106.5 ± 4.32	7.7 ± 0.28	13.8
26	89.6 ± 3.22	1.3 ± 0.03	68.9
29	177.3 ± 4.70	26.5 ± 1.20	6.70
30	140.7 ± 1.9	2 ± 0.3	70.3
31	80 ± 7.50	18.8 ± 2.80	4.20
32	86 ± 3.50	8.5 ± 1.00	10.10
33	78.7 ± 3.60	0.3 ± 0.04	262
(*S*)-ibuprofen	3.2	1.5	2.10
NS398 [0.2 μM]	14.1	73.2	0.19
celecoxib	6.86	0.10	69
rofecoxib	23.5	0.78	30.12

[a] Results are expressed as the mean (n = 3) of the % inhibition of PGH_2 production by test compounds with respect to control samples. In vitro COX-2 selectivity index is IC_{50}(COX-1)/IC_{50}(COX-2). ND: not determined.

Compounds **20**, **26**, **33**, **9**, and **30** were the most potent in inibiting the in vivo inflammation induced by carrageenan, compared to the action of ibuprofen. In contrast **10**, **22**, and **12** showed less anti-inflammatory activity than ibuprofen in the rat paw edema assay.

A comparison of data revealed that **20**, **26**, **33**, **9**, and **30** showed significantly longer anti-inflammatory activity than ibuprofen. Ibuprofen showed a considerable reduction in anti-inflammatory activity 4 h after carrageenan administration, while the activity of **20**, **26**, and **33** practically did not change between 4 and 5 h after the administration of product. Therefore, **20**, **26**, and **33** could be considered for the potential development of new AINEs with anti-inflammatory activity.

Regarding structure−activity relationships, **20** showed the strongest anti-inflammatory activity. Replacement of the thiophene group by furan, such as in compound **9**, decreased the anti-inflammatory activity of the arylmethylsulfone moiety. The presence of substituents on the aryl group (**12**, **13**, **22**, and **29**) decreased the anti-inflammatory activity of **20** compared to compounds containing a heterocyclic ring (**20**, **26**, and **33**). The thiophene nucleus in **20** showed greater anti-inflammatory activity in vivo than the pyridine moiety in **26**.

Our results on biological activity indicate that the introduction of 2-thiophene to the arylsulfones is relevant, as **20** showed more activity than the analogue **9**, which has a furan ring. The nature of the heterocyclic aromatic on the *p*-position of the methyl sulfone phenyl had a strong effect on anti-inflammatory activity. The methylsulfone **20**, a highly potent anti-inflammatory with a diarylketone scaffold, could be considered suitable for a future generation of COX inhibitors. This compound presented reasonable oral bioavailability compared with the other compounds of the same series.

Table 2. Anti-Inflammatory Activity of the Compounds in Vivo (Edema Induced by Carrageenan)[a]

	3 h		4 h	
compd	swelling	% inhibition	swelling	% inhibition
20	(a) 17.5 ± 5.6***	59.7	(a) 19.1 ± 5.3***	56.0
	(b) 43.4 ± 6.9		(b) 43.4 ± 8.4	
26	(a) 20.1 ± 4.9***	53.7	(a) 21.1 ± 5.5***	51.4
	(b) 43.4 ± 6.9		(b) 43.4 ± 8.4	
33	(a) 22.8 ± 4.5***	48.7	(a) 24.1 ± 5.1***	46.0
	(b) 43.4 ± 6.9		(b) 43.4 ± 8.4	
9	(a) 28.3 ± 5.6***	45.5	(a) 30.0 ± 4.4**	37.8
	(b) 51.9 ± 6.8		(b) 48.2 ± 7.7	
30	(a) 31.7 ± 5.6***	41.9	(a) 25.2 ± 3.6**	32.6
	(b) 54.5 ± 6.8		(b) 38.9 ± 2.3	
10	(a) 37.9 ± 4.8**	27.0	(a) 37.5 ± 5.7*	22.2
	(b) 51.9 ± 6.8		(b) 48.2 ± 7.7	
22	(a) 40.5 ± 5.6**	22.0	(a) 44.3 ± 4.6	8.1
	(b) 51.9 ± 6.8		(b) 48.2 ± 7.7	
12	(a) 32.2 ± 5.1*	13.7	(a) 34.9 ± 5.0	4.4
	(b) 37.3 ± 3.1		(b) 36.5 ± 4.3	
13	NA		NA	
29	NA		NA	
ibuprofen	(a) 27.1 ± 3.6***	30.3	(a) 34.4 ± 6.9**	23.9
	(b) 38.9 ± 6.0		(b) 45.1 ± 5.0	

[a] (a) Swelling for a dose of 70 mg/kg. (b) Swelling control. NA no activity attributable to low solubility in water. Values significantly differ from controls as indicated: ∗, $P < 0.05$; ∗∗, $P < 0.01$; ∗∗∗, $P < 0.001$; #, does not differ significantly according to unpaired one-tailed Student's *t*-test. The data represent the mean ± SEM of six animals ($p < 0.05$). The rat paw edema occurred at 3 and 4 h after carrageenan administration.

Effect of Compounds on Cell Viability. The antiproliferative activities of compounds **9**−**13**, **20**−**22**, and **29**−**33** were evaluated against the following cell lines: K562 (leukemia-lymphoma), NCI-H460 (human nonsmall lung carcinoma) and HT29 (human colon cancer). We used the trypan blue dye exclusion assay and MTT for this purpose. Antitumor activities were compared with celecoxib (anti-inflammatory) and purvalanol A (specific inhibitor of cyclin-dependent kinase activities).

Treatment of K562 cells with **9**−**13**, **20**−**22**, and **29**−**33** at 10 μM did not affect cell viability, and the effects were relatively poor (Table 3).

Treatment of NCI-H460 cells with 10 μM pyrrole derivative **13** resulted in a decrease in cell viability of 54.8 ± 0.70%. In addition, treatment with 10 μM other compounds had no cytotoxic effect, while 100 μM **12**, **22**, **29**, **30**, **31**, and **33** showed poor cytotoxicity with a mean of growth inhibition of 22.0%, 20.3%, 42.8%, 43.2%, 27.7%, and 27.3%, respectively.

Finally, treatment of HT-29 with 10 μM compounds **9**−**13**, **20**−**22**, and **29**−**33** did not have a significant effect on cell viability. The IC_{50} ranged from 34 (compound **12**) to 383 (compound 9) μM (Table 3).

To examine the effects of compounds **9**−**13**, **20**−**22**, and **29**−**33** on primary culture, HuDe cells were treated with 100 μM test compounds. At this tested concentration none of the compounds showed a significant effect on cell viability except **12** (Table 3).

SAR of Arylsulfones. A comparison of these structures indicated that the presence of the *N*-(2-fluorophenyl)pyrrole subunit resulted in greater cytotoxicity than that of other aromatic rings. The presence of an aroyl group at the C-2 position of the pyrrole (**12**) produced greater activity against HT-29 and HuDe cells than the corresponding isomer of position (**13**). Compound **13**, with the aroyl group at the C-3 position, showed considerable capacity to inhibit H-460 cell growth. The carbonyl linkage that acts as spacer between the two aryl rings offers the possibility of adopting a conformation that is suitable for interaction with the site active. The 3-substituted furan (**10**) and the 3-substituted thiophene (**21**) exhibited slightly more inhibitory activity in HT-cell than

Table 3. Inhibition of K562, NCI-H460, and HT-29 Cancer Cells and HuDe Cell Proliferation[a]

	% inhibition [10 μM]		% inhibition [100 μM]	IC_{50} (μM)
compd	K562 cell viability	NCI-H460 cell viability	HuDe cell viability	HT-29 cell viability
9	8.3 ± 0.50	3.0 ± 0.70	30.7 ± 6.40	383.0 ± 6.40
10	8.3 ± 1.00	6.0 ± 1.00	36.2 ± 2.00	104.0 ± 1.60
11	2.1 ± 0.20	7.0 ± 0.01	30.8 ± 1.70	70.4 ± 0.50
12	2.1 ± 0.02	13.3 ± 0.50	45.0 ± 2.10	34.1 ± 2.10
13	12.5 ± 1.00	54.8 ± 0.70	13.4 ± 0.90	96.1 ± 1.00
20	1.0 ± 0.10	3.0 ± 0.40	25.7 ± 2.80	122.0 ± 2.10
21	14.6 ± 2.00	2.0 ± 0.09	31.2 ± 0.40	75.7 ± 9.00
22	6.2 ± 0.10	12.7 ± 1.90	29.4 ± 0.05	100.0 ± 8.40
29	13.5 ± 3.90	6.6 ± 0.08	12.3 ± 1.00	100.0 ± 1.20
30	13.5 ± 0.60	1.8 ± 0.01	37.4 ± 1.90	130.0 ± 5.20
31	17.7 ± 2.00	3.1 ± 0.20	36.1 ± 0.80	65.8 ± 4.70
32	1.0 ± 0.05	3.0 ± 0.30	28.9 ± 2.00	146.4 ± 7.90
33	16.6 ± 0.90	12.2 ± 1.00	34.3 ± 0.70	85.0 ± 5.70
celecoxib	38.8 ± 2.00	9.75 ± 1.10	92.0 ± 1.60	45.5 ± 0.90
purvalanol A	75.1 ± 2.30	3.98 ± 0.10	88.6 ± 1.90	≫100

[a] Cancer cell viability on K-562 and H-460 after treatment with 10 μM **9**−**13**, **20**−**22**, and **29**−**33**. Cell viability is on human derm fibroblasts (HuDe) after treatment with 100 μM. Values represent [control (DMSO) − treated] /control (DMSO) and are expressed as average values of two separate experiments repeated in duplicate. HT-29 cell viability is for after treatment with a range of concentrations of compounds **9**−**13**, **20**−**22**, and **29**−**33**. IC_{50} values are expressed as average values of two separate experiments repeated four times. Purvalanol: Sigma-Aldrich, ref P4484. Celecoxib: LC Laboratories, ref 1502.

Table 4. MD (debye), Experimental Activity (ΔG_{bind}), Free Energy of Solvation (ΔG_{solv}), and Calculated Binding Affinity (ΔG_{bind}(MM-GBSA)) of Compounds **9**−**14**, **20**−**23**, **26**, and **29**−**33**

MD (D)	ΔG_{bind} (kcal/mol)	ΔG_{solv} (kcal/mol)	IC_{50}(COX-2) in vitro (μM)	compd	ΔG_{bind}(MM-GBSA) (kcal/mol)
8.333	−6.41	−10.27	19.2	**9**	−26.1 ± 2.0
7.226	−7.32	−10.71	4.1	**10**	−24.87 ± 2.0
6.348	−6.02	−12.42	36.8	**11**	−30.55 ± 3.5
8.028	−5.93	−10.32	43.3	**12**	−38.96 ± 3.1
8.571	−6.39	−10.73	19.7	**13**	−44.86 ± 2.5
6.084	−6.83	−15.96	9.4	**14**	−35.13 ± 2.4
8.398	−6.30	−10.48	23.1	**20**	−26.36 ± 2.7
7.480	−6.55	−10,76	15.2	**21**	−27.95 ± 2.3
6.121	−8.15	−9.57	1.0	**22**	−38.25 ± 1.5
8.344	−6.95	−9.48	7.7	**23**	−34.35 ± 2.1
7.933	−8.00	−9.45	1.3	**26**	−32.94 ± 1.8
7.979	−6.22	−10.99	26.5	**29**	−28.12 ± 1.7
7.350	−7.74	−11.55	2.0	**30**	−34.98 ± 1.6
6.234	−6.42	−10.38	18.8	**31**	−31.86 ± 1.9
5.657	−6.89	−9.47	8.5	**32**	−30.74 ± 1.9
5.084	−8.86	−9.39	0.3	**33**	−37.65 ± 1.4

that shown by corresponding 2-substituted isomers. The indole derivative **33** showed greater activity than the pyrrole analogue (**32**). The piperazine-arylsulfone (**31**) exhibited modest growth inhibition of HT-29 cells but was superior to the effect of the diarylamine (**30**). In contrast **22** and **29** which had distinct structural characteristics showed similar and modest cytotoxicity. The cytotoxic activity of the compounds series at the concentrations tested was not sufficient to inhibit cancer cell proliferation; however, in a time-dependent manner, these compounds may concentrate in cancer tissue and exert cumulative effects. Clinical studies have indicated that a dose of 400 mg b.i.d. of celecoxib reduces polyp growth while this effect was insignificant at 100 mg b.i.d. and rofecoxib does not show antitumor activity even at relatively high doses. Molecular modeling studies may explain these effects and also contribute to the design of novel compounds that provide either a more specific COX inhibitor or potent inhibitor of cancer cell proliferation.

QSAR Analysis. The optimized geometries for the 16 methyl sulfone derivatives were obtained at the B3LYP/6-31G(d) level, and the relative free energies of hydration were calculated using the MST B3LYP/6-31G(d) version of the PCM continuum model.

Physicochemical parameters were examined in order to find a possible explanation for the observations described above and to provide a better understanding of the relationship between structure and anti-inflammatory activity. The dipole moment and the energies of the NHOMO and NLUMO orbitals in aqueous solution for the 16 compounds were studied.

The dipole moment plays an interesting role in aligning optimally with the receptor. The orientation and magnitude of the dipole moment are crucial for the COX-2 inhibition activity[22] (**9** and **10**) (Figure 2A in Supporting Information).

A statistically significant correlation ($n = 11$, $r^2 = 0.808$) was observed between COX-2 inhibition ($\Delta G_{bin} = -RT \ln(1/IC_{50})$ and dipole moment. However, 5 compounds (**11**, **14**, **26**, **31**, and **32**, outlying points) showed very large free energy of solvation or the HOMO delocalized over aromatic rings. For these compounds, the magnitude of the dipole moment established a worse relation with capacity to inhibit COX-2 than the same potent compounds of this series (Table 4).

The electron density maps of the HOMO and NHOMO orbitals appear to be centered in the phenyl, thiophene, or *N*-indole group, exhibiting a π-character, on the most active compounds (**33**, **22**, **30**, and **26**) (Figure 2B in Supporting Information), with the exception of **32** and **10**. However, the HOMO was delocalized over aromatic rings on the less active compounds (**12**, **29**). The NHOMO was located at the thiophene or pyrrole ring, and the NLUMO was delocalized over the whole structure on the compounds that showed the most effective inhibition (**12**, **21**) (Figure 2C in Supporting Information) of human cancer (HT-29) cell proliferation in vitro.

Molecular Modeling Studies. Visual inspection of the complex of methyl sulfone derivatives and COX-2 (Figure 3) revealed the same binding orientation as that observed for the carboxylic group of flurbiprofen in COX-2 (3PGH). This orientation involved hydrogen bonding interactions of the oxygen atoms of the sulfone group at the mouth of the binding channel with Arg120 and Tyr355. Furthermore, Val349, Phe518, and Leu352 were within van der Waals contact. Additional hydrogen bonds were observed between the oxygen atom of the carbonyl group and the hydroxyl groups of Ser530.

These studies demonstrate that the sulfone group of these nonsteroidal anti-inflammatory drugs bind to COX enzyme in an orientation that precludes the formation of hydrogen bonding with Arg120, Ser353, and Tyr355 through their oxygen atoms. Further relevant hydrophobic interactions were observed in a top cavity formed by Phe518, Leu384, Tyr385, and Trp387. Hydrophobic residues Leu352, Ala527, and Val523 surrounded the phenyl ring.

Also the CH_3 of the methylsulfone group was bound to an adjacent pocket formed by Met113, Val116, Val349, and Leu531. Finally, the oxygen atom of the carbonyl group formed hydrogen bonds with Ser530.

Compounds **33**, **32**, and **26**, which showed potent inhibitory activity of COX-2 in vitro and anti-inflammatory activity in vivo, interacted with COX-2 via one of the oxygen atoms of the sulfone group with Arg120 and Tyr355 (Figure 4).

An additional hydrogen bonding interaction was observed between one of the oxygen atoms of its sulfone group and Ser353. Further multiple hydrophobic contacts involving the Leu352, Ala527, and Val523 were observed. Also, the indole group was in close van der Waals contacts with Leu384 and Trp387 only for **33**. However, notable differences were detected in the relative arrangement of the indole ring compared to the position occupied by the corresponding moiety of pyrrole or pyridine ring. This arrangement thus led to a more efficient $\pi-\pi$ stacking interaction between the indole ring of **33** and the phenyl ring of Phe518.

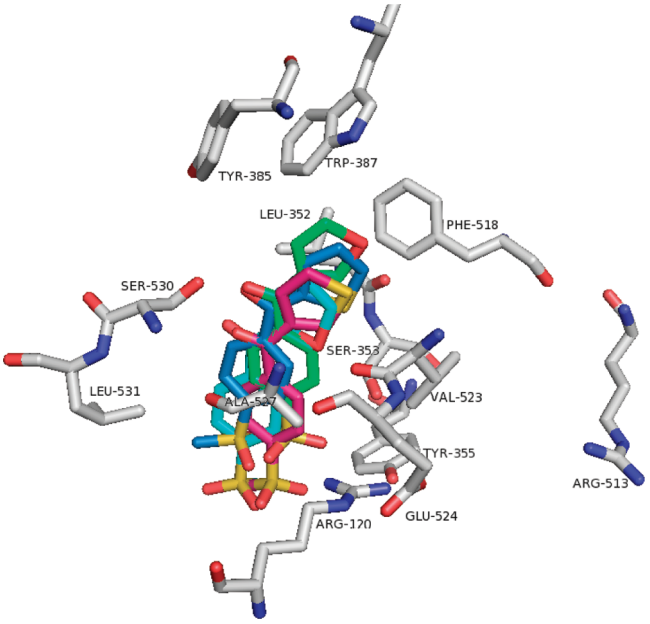

Figure 3. Superposition representation of the thiophene and furane methylsulfone derivatives (**9** (light blue), **10** (green), **20** (blue), and **21** (brown)) in the binding site of mouse COX-2, highlighting selected residues that form the main interactions of the inhibitors. Most hydrogen atoms are omitted for the sake of clarity.

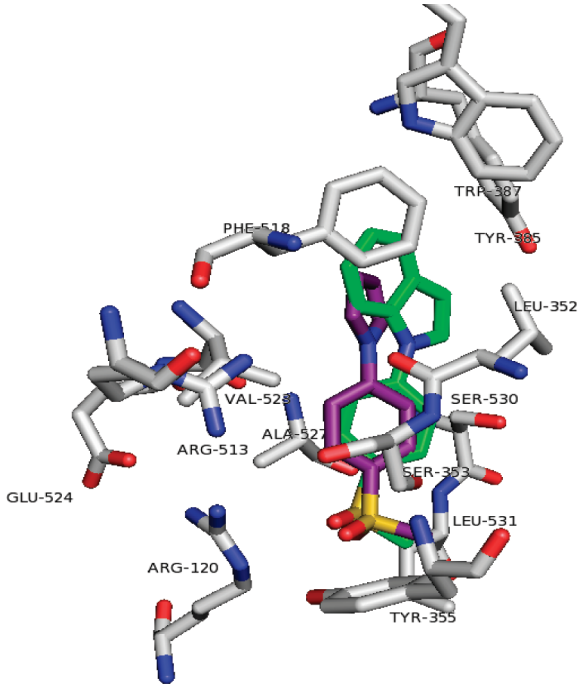

Figure 4. Superposition of the *N*-arylpyrrole and *N*-arylindole methylsulfone derivatives (**32** (violet) and **33** (green)) in the binding site of mouse COX-2, highlighting selected residues that form the main interactions of the inhibitors. Most hydrogen atoms are omitted for the sake of clarity.

Thiophene and furan derivates (**9**, **10**, **20**, and **21**) formed hydrogen bonds with COX-2 via one of the oxygen atoms of the sulfone group with Arg120 and Ser353 (except **21**, which formed a hydrogen bond with Tyr355 (Figure 3). A few hydrophobic contacts were observed close to Ile345, Val349, Leu352, and Val523 for these compounds.

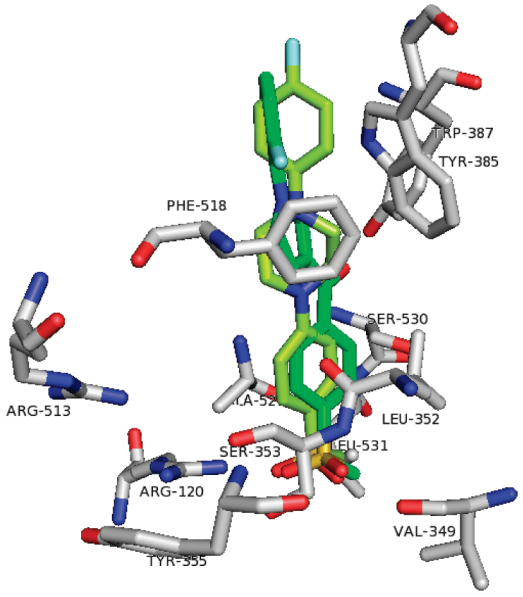

Figure 5. Superposition of the triphenyl methylsulfone derivatives (**13** (green) and **31** (light green) compounds) in the binding site of mouse COX-2, highlighting selected residues that form the main interactions of the inhibitors. Most hydrogen atoms are omitted for the sake of clarity.

The orientation and magnitude of the dipole moment on these compounds are very crucial for their best docked position in the COX-2 binding pocket in such a way that the π−aromatic contacts involving Phe518 and Trp387 are revealed. Analysis of the MM-GBSA computations of the binding free energy and dipole moments showed a close relation ($n = 13$, $r^2 = 0{,}746$).

Compounds **13** and **31**, which are active in the antitumor bioassay, and shown the same anti-inflammatory activity, interacted with COX-2 in a distorted mode compared to the other compounds. This interaction occurred via the binding of one hydrogen atom with Arg120 through its sulfone group (Figure 5). Additional hydrophobic contacts with the methylsulfone phenyl ring involving Ile345, Val359, Ala527, and Leu531 were detected.

The main hydrophobic interactions were found in a top cavity formed by Phe518, Leu384, Tyr385, and Trp387.

Analysis of the complexes of compounds **12** and **29** (less active) in their docked position with COX-2 (Figure 6 in Supporting Information) revealed hydrogen bonds of the former involving the oxygen atoms of the sulfone group with Arg120 and with Ser353.

Also, the benzoxazine or pyrrole groups were in close van der Waals contact with Leu352, Phe518, and Ala527 while the fluorophenyl ring showed an inversed binding orientation compared to **29** and displacement of Tyr385.

Compounds **22**, **23**, and **30**, which showed the same anti-inflammatory activity, interacted with COX-2 via one of the oxygen atoms of the sulfone group with Ser353 and Tyr355 at the mouth of the channel, and the oxygen atom of the carbonyl/amine moiety formed hydrogen bonds with Ser530 (Figure 7 in Supporting Information). Additional hydrophobic contacts involving Ile345, Val359, Ala527, and Leu531 were observed with the methylsulfonephenyl ring. However, in **22** and **23** the methylsulfone group was slightly rotated. The main hydrophobic interactions were observed in a top cavity formed by Leu384, Tyr385, and Trp387. Finally, the

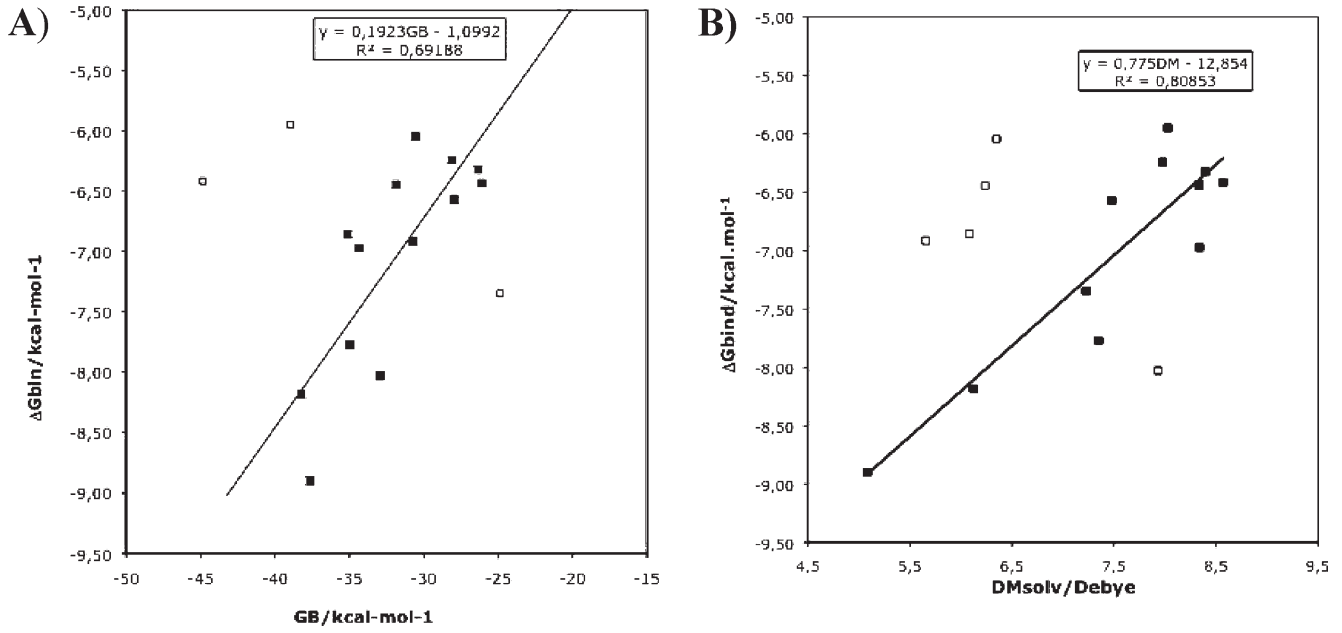

Figure 9. (A) Correlation ($n = 13$, $r^2 = 0.69$) between COX-2 experimental inhibition activity (ΔG_{bind}) and calculated ΔG_{bind}(GBSA) and (B) correlation ($n = 10$, $r^2 = 0.808$) between experimental inhibitory activity of COX-2 (ΔG_{bind}) and dipole moment (DM).

fluoro-/bromophenyl rings were roughly stacked onto the aromatic ring of Phe518.

However, the best docked position of **14** and **11** with COX-2 (Figure 8 in Supporting Information) showed the oxygen atoms of the sulfone moiety hydrogen-bonded to Tyr355, Arg120, and Ser353 at the mouth of the channel, and the oxygen atom of the carbonyl formed hydrogen bonds with Ser530. Also, the indole group was in close van der Waals contact with Leu384, Trp387, and Phe518; however, **11** showed notable differences in the relative arrangement of the indole ring through the methyl group compared to **14**.

The calculation of binding free energy, ΔG_{bind}(MM-GBSA), between protein and ligands was evaluated using GBSA. Statistically significant correlations ($n = 13$, $r^2 = 0.69$) were observed between experimental ΔG_{bin} and calculated ΔG_{bind}(GBSA) (Figure 9A).

The orientation and magnitude of the dipole moment on these compounds are highly relevant for their the best docked position in the COX-2 binding pocket, as it reveals π−aromatic contacts involving Phe518 and Trp387. Statistically significant correlations ($n = 10$, $r^2 = 0.808$) were observed between COX-2 inhibition activity and dipole moment (Figure 9B). The main hydrophobic interactions observed in a top cavity formed by Leu384, Tyr385, Trp38, and Phe518 could explain the notable differences in the relative anti-inflammatory activity of these compounds (Figure 10).[23]

In summary, here we have described a straightforward and efficient synthesis of new anti-inflammatory compounds containing an arylcarbonyl or an aryl group at the para position of the pharmacophoric methylsulfonephenyl group. The compounds synthesized showed anti-inflammatory and cytotoxic activities of diverse intensity. Compound **20** had the strongest in vivo anti-inflammatory activity which exceeds (2- and 2.4-fold at 3 and 4 h after the administration of carrageenan, respectively) that of the parent reference, ibuprofen, followed by **26**, **33**, **9**, and **30** which showed more activity than ibuprofen 3 and 4 h after administration. Our findings may contribute to the future construction of a pharmacophoric model of COX-2 inhibitors and pave the way for further research involving structures with a low dipolar moment and minimum free energy of solvation. Our results indicate that a simple methylsulfone with an aryl group involved in the affinity and in the activity showed interesting anti-inflammatory activity by inhibiting COX and weak cytotoxic. This study may suggest that these compounds possess the correct electronic density and the dipole moment directionality to an important COX-2 receptor affinity.

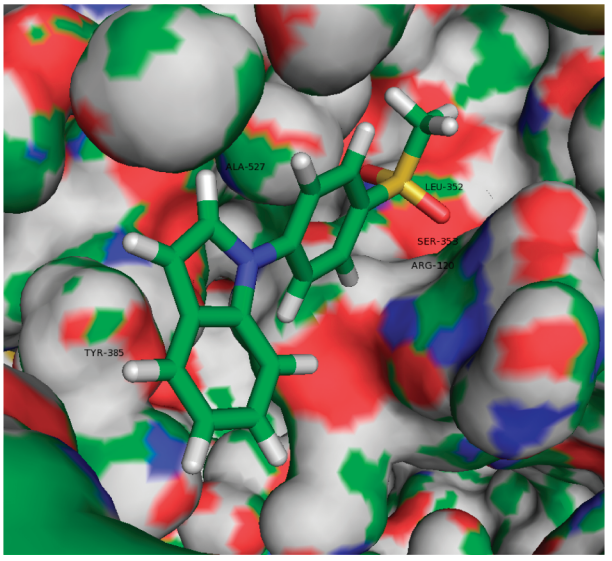

Figure 10. Compound **33** found in its respective complex with COX-2. Relevant active site residues for one representative protein are shown. A solid solvent-accessible surface envelops the side chains of the labeled residues (except Phe518, Trp387, and Ser530) to delineate the active site cavity. Water molecules and the hydrogen atom have been omitted for clarity.

Experimental Section

(A) Chemical. General. Melting points were obtained on an MFB-595010M Gallenkamp apparatus in open capillary tubes and are uncorrected. IR spectra were obtained using a FTIR

Perkin-Elmer 1600 infrared spectrophotometer. Only noteworthy IR absorptions are listed (cm^{-1}). ^1H and ^{13}C NMR spectra were recorded on a Varian Gemini-200 (200 and 50.3 MHz, respectively) or Varian Gemini-300 (300 and 75.5 MHz) instrument using $CDCl_3$ as solvent with tetramethylsilane as internal standard or $(CD_3)_2CO$. Other ^1H NMR spectra and heterocorrelation $^1H-^{13}C$ (HMQC and HMBC) experiments were recorded on a Varian VXR-500 (500 MHz). Mass spectra were recorded on a Helwett-Packard 5988-A. Column chromatography was performed with silica gel (E. Merck, 70−230 mesh). Reactions were monitored by TLC using 0.25 mm silica gel F-254 (E. Merck). Microanalysis was determined on a Carlo Erba 1106 analyzer. All reagents were of commercial quality or were purified before use. Organic solvents were of analytical grade or were purified by standard procedures. Commercial products were obtained from Sigma-Aldrich. Elemental analysis was used to ascertain purity of >95% for all compounds of this work for which biological activities were determined.

General Method for the Preparation of the Diarylalcohols and Oxidation to Ketones. (**A**) To a solution of the bromothioanisole (450 mg, 2.22 mmol) in THF (4 mL) was added a solution of *n*-BuLi in hexane (1.4 mL, 2.22 mmol) at −78 °C under an argon atmosphere. The mixture was stirred at the same temperature for 1 h. Then a solution of the corresponding aldehyde or ketone (2.50 mmol) in freshly distilled THF (2 mL) was added, and the mixture was allowed to warm slowly to 20 °C. At this time a solution of saturated NH_4Cl was added (3 mL), and the mixture was stirred for 20 min. Finally it was extracted with ether (3 × 20 mL) and the aqueous phase was acidified with 2 N HCl and extracted with CH_2Cl_2 (3 × 20 mL). The organic layers were dried (Na_2SO_4), filtered, and concentrated under vacuum, and the crude product was purified by silica gel column chromatography. Using a mixture of hexane/ethyl acetate (5:95) as eluent, the desired alcohol was obtained.

(**B**) The intermediate alcohol (1 mmol) was rapidly treated with MnO_2 (3 mmol) in dichloromethane (15 mL). The reaction mixture was stirred for 12 h at room temperature. The crude of reaction was filtered, washed with dichloromethane, and the solvent was removed in rotator evaporator. The obtained residue was purified by silica gel column chromatography using 8:2 hexane/ethyl acetate mixture as eluent.

2-(*p*-Methylthiophenylhydroxymethyl)furan (2a). By use of the above-described procedure, the furan-2-carbaldehyde was converted to the title alcohol as oil in 92% yield. The crude of reaction obtained was rapidly oxidized with MnO_2 because of high instability.

***N*-(2-Fluorophenyl)-2-(*p*-methylthiophenylhydroxymethyl)pyrrole (2d).** Starting from *p*-bromothioanisole (450 mg, 2.22 mmol) and *N*-(2-fluorophenyl)pyrrole-2-carbaldehyde (**23**) (350 mg, 1.85 mmol), following the procedure described above, and using 1.6 M BuLi in THF (1.38 mL, 2.22 mmol) at −78 °C, the corresponding diarylmethanol was obtained. The carbynol was extracted with ether (3 × 25 mL), dried over Na_2SO_4, filtered off, and the solvent was removed under vacuum. The intermediate carbynol was obtained with sufficient purity to go to the new step of oxidation to the ketone using MnO_2. The title compound was obtained as a colorless oil after purification by column chromatography, eluting with a mixture of hexane/ethyl acetate 80:20 (520 mg, 1.66 mmol) in a 90% yield. IR (KBr), δ (cm^{-1}): 3220 (OH); 1180 (C−O); 1091 (C−S). ^1H NMR ($CDCl_3$, 200 MHz) δ (ppm): 2.47 (s, 3H, CH_3-); 5.60 (d, J = 4 Hz, 1H, CH-O), 6.08 (m, 1H, C-4H); 6.28 (m, 1H, C-3H); 6.78 (m, 1H, C-5H); 7.22 (m, 8H, Ar). The crude of reaction was rapidly oxidized with MnO_2 because of high instability.

2-(*p*-Methylthiobenzoyl)furan (3). Starting from the *p*-bromothioanisole (500 mg, 2.46 mmol) and the furfural (196.8 mg, 2.05 mmol), following the procedure described before, and using BuLi in THF at −78 °C, the corresponding diarylmethanol was obtained, which was of sufficient purity to go to the new step of oxidation to the ketone using MnO_2. The title compound was obtained as a white solid (406 mg, 1.87 mmol) in a 91% yield. Mp: 81−83 °C (hexane/ethyl acetate). IR (KBr), ν (cm^{-1}): 1633 (CO); 1296 (Ar−O); 1091 (C−S). ^1H NMR ($CDCl_3$, 200 MHz) δ (ppm): 2.54 (s, 3H, CH_3-); 6.59 (m, 1H, C-4H), 7.23 (m, 1H, C-3H); 7.30 (d, J = 8.4 Hz, 2H, C-3′H and C-5′H); 7.69 (m, 1H, C-5′H); 7.94 (d, J = 8.4 Hz, 2H, C-2′H and C-6′H). ^{13}C NMR ($CDCl_3$, 50.3 MHz) δ (ppm): 14.8 (CH_3, CH_3-); 112.1 (CH, C-4); 119.9 (CH, C-3); 124.8 (CH, C-3′ and C-5′); 129.8 (CH, C-2′and C-6′); 133.2 (C, C-1′); 145.4 (C, C-2); 146.8 (CH, C-5); 152.3 (C, C-4′); 182.4 (C, CO).

General Method for the Preparation of Diarylketones. A stirred solution of thioanisole (127 mg, 1.02 mmol) in dry dichoromethane (15 mL) was cooled to 0 °C under argon atmosphere. The solution was stirred vigorously, and a solution of titanium tetrachloride (0.15 mL, 1.36 mmol) was added slowly. A solution of the corresponding carboxylic chloride (0.80 mmol) in dichloromethane (2 mL) was added to the mixture. The reaction mixture was stirred for 10 h at room temperature. The crude of reaction was poured into 40 mL of ice−water, and the aqueous layer was separated. The organic layer was washed with saturated $NaHCO_3$, dried over Na_2SO_4, and evaporated to afford a residue which was purified by column chromatography using 8:2 hexane/ethyl acetate.

2-(*p*-Methylthiobenzoyl)thiophene (16). The title compound was obtained as a white solid from 2-thiophene carboxylic chloride and thioanisole following the above-described conditions in 50% yield after purification by column chromatography. Mp: 64−66 °C (hexane/ethyl acetate). IR (KBr), ν (cm^{-1}): 1622 (C═O); 1088 (S−CH_3). ^1H NMR ($CDCl_3$, 200 MHz) δ (ppm): 2.54 (s, 3H, CH_3−S); 7.16 (dd, J_1 = 5.2, J_2 = 3.6 Hz, 1H, C-4H); 7.31 (d, J = 8.8 Hz, 2H, C-3′H y C-5′H); 7.64 (dd, J_1 = 3.8, J_2 = 1 Hz, 1H, C-3H); 7.71 (dd, J_1 = 5.2, J_2 = 1 Hz, 1H, C-5H); 7.82 (d, J = 8,8, 2H, C-2′H y C-6′H). ^{13}C NMR ($CDCl_3$, 50.3 MHz) δ (ppm): 14.8 (CH_3, CH_3−); 124.8 (CH, C-3′ y C-5′); 127.7 (CH, C-4); 129.6 (CH, C-2′ and C-6′); 133.7 (CH, C-3); 133.9 (C, C-1′); 134.1 (CH, C-5); 143.4 (C, C-2); 144.9 (C, C-4′); 186.9 (C, CO).

General Procedure for the Oxidation of Methylthio Derivatives to Sulfones. To a solution of the methylthio derivative (100 mg, 0.34 mmol) in 25 mL of dry dichloromethane cooled at 0 °C, *m*-CPBA (129 mg, 0.75 mmol) was slowly added. The reaction mixture was stirred at room temperature for 4 h. After the mixture was treated with a solution of 2 N NaOH (3 × 25 mL), the organic layer was separated and dried over anhydrous sodium sulfate, filtered off, and the solvent was removed by evaporation. The residue was then purified by silica gel column chromatography, eluting with a mixture 7:3 hexane/ethyl acetate.

2-(*p*-Methylsulfonylbenzoyl)furan (9). From the corresponding methylthio derivative (218.27 mg, 1 mmol) and following the general procedure described above, the title compound was obtained (207.1 mg, 0.95 mmol) as a white powder in 95% yield. Mp: 96−98 °C (hexane/ethyl acetate). IR (KBr), ν (cm^{-1}): 1642 (CO); 1434 (SO_2); 1278 (Ar−S); 1099 (C−O). ^1H NMR ($CDCl_3$, 200 MHz) δ (ppm): 3.11 (s, 3H, CH_3-S); 6.62 (m, 1H, C-4H); 7.31 (m, 1H, C-3H); 7.79 (s,1H, C-5H); 8.13 (d, J = 5.6 Hz, 4H, C-2′H, C-3′H, C-5′H and C-6′H). ^{13}C NMR ($CDCl_3$, 50.3 MHz) δ (ppm): 44.4 (CH_3, CH_3-); 112.7 (CH, C-4); 121.4 (CH, C-3); 127.4 (CH, C-3′, and C-5′); 130.0 (CH, C-2′, and C-6′); 141.5 (C, C-1′); 143.4 (C, C-2); 147.8 (CH, C-5); 151.7 (C, C-4′); 180.6 (C, CO). Anal Calcd for $C_{12}H_{10}NO_4S$: C, 57.59%; H, 4.03%. Found: C, 57.21%; H, 4.42%.

2-(*p*-Methylsulfonylbenzoyl)thiophene (20). From the corresponding methylthio derivative (120 mg, 0.51 mmol) and following the general procedure described above, the title compound was obtained (100 mg, 0.37 mmol) as a white powder in 73% yield. Mp: 136−138 °C (hexane/ethyl acetate). IR (KBr), ν (cm^{-1}): 1636 (CO); 1413 (SO_2); 1286 (Ar−S); 1154 (SO_2). ^1H NMR ($CDCl_3$, 200 MHz) δ (ppm): 3.13 (s, 3H, CH_3−S); 7.20 (dd, J_1 = 4.8, J_2 = 3.6 Hz, 1H, C-4H); 7.62 (dd, J_1 = 3.6, J_2 = 1 Hz, 1H, C-3H); 7.81 (dd, J_1 = 4.8, J_2 = 1 Hz, 1H, C-5H); 8.05

(dd, J_1 = 8.4, J_2 = 1 Hz, 4H, C-2′H, C-3′H, C-5′H y C-6′H). ^{13}C NMR ($CDCl_3$, 50.3 MHz) δ (ppm): 44.3 (CH_3, CH_3-); 127.5 (CH, C-3′ and C-5′); 128.3 (CH, C-4); 129.7 (CH, C-2′ and C-6′); 135.4 and 135.5 (CH, C-3, and C-5); 142.5 and 142.6 (C, C-2 and C-1′); 143.2 (C, C-4′); 186.5 (C, CO). Anal Calcd for $C_{12}H_{10}O_3S_2$: C, 54.11%; H, 3.78%. Found: C, 53.86%; H, 3.64%.

General Procedure for Obtaining Diaryl Compounds. A suspension of bromoaryl (2.46 mmol), bromopyridine (387 mg, 2.46 mmol), Cu (134 mg, 3.69 mmol), and anhydrous K_2CO_3 (509 mg, 3.69 mmol) without solvent in a Schlenk tube was heated at 300 °C for 8 h. At this time, the reaction mixture was poured into 25 mL of water and was extracted with ether (3 × 30 mL). The organic phase was dried and evaporated at vacuum to yield colorless oil. The residue was purified by silica gel column chromatography, eluting with 8:2 hexane/ethyl acetate.

2-(*p*-Methylthiophenyl)pyridine (25). Starting from (500 mg, 2.46 mmol) of 4-bromothianisole and following the general procedure described before, the title compound was obtained as a white solid (50 mg, 0.25 mmol) in 10% yield. Mp: 55−57 °C (hexane/ethyl acetate). IR (KBr), ν (cm^{-1}): 1584 (C═C); 1463 (C═C), 843 C−S). ^{1}H NMR ($CDCl_3$, 200 MHz) δ (ppm): 2.53 (s, 3H, CH_3-); 7.20 (m, 1H, H−Ar); 7.40 (d, J = 8.8 Hz, 2H, C-2′H and C-6′H); 7.68 (m, 2H, H-pyridine); 7.91 (d, J = 8.8 Hz, 2H, C-3′H and C-5′H); 8.65 (m, 1H, C-6H pyridine).

2-(*p*-Methylsulfonylphenyl)pyridine (26). Starting from (50 mg, 0.25 mmol) of the corresponding methylthio compound and following the general procedure described before, the title compound was obtained as a white solid (35 mg, 0.15 mmol) in 60% yield. Mp: 86−88 °C (hexane/ethyl acetate). IR (KBr), ν (cm^{-1}): 1300 (SO_2); 1152 (S−O). ^{1}H NMR ($CDCl_3$, 200 MHz) δ (ppm): 3.10 (s, 3H, CH_3-); 7.28 (m, 1H, C-5H), 7.81 (m, 2H, C-3H, and C-4H); 8.02 (d, J = 8.8, 2H, C-2′H, and C-6′H); 8.07 (d, J = 8.8, 2H, C-3′H, and C-5′H); 8.73 (d, J = 5.5, C-6H). ^{13}C NMR ($CDCl_3$, 50.3 MHz) δ (ppm): 44.6 (CH_3, CH_3-); 121.1 (CH, C-3); 123.4 (CH, C-5); 127.7 (CH, C-2′ and C-6′); 127.8 (CH, C-3′and C-5′); 137.1 (CH, C-4); 140.4 (C, C-1′); 144.4 (C, C-4′); 149.9 (CH, C-6); 155.1 (C, C-2). Anal Calcd for $C_{12}H_{11}NO_2S$: C, 61.78%; H, 4.75%; N, 6.00%. Found: C, 61.63%; H, 4.65%; N, 6.17%.

Preparation of 1,4-Benzoxazines 4-(*p*-Methylthiophenyl)-4*H*-pyrrolo[2,1-*c*][1,4]benzoxazine (28). To a solution of *N*-(2-fluorophenyl)-2-((*p*-methylthiophenyl)hydroxymethyl)pyrrole (**2d**) (500 mg, 1.59 mmol) in dry DMF (5 mL) was added (127 mg, 3.18 mmol) sodium hydride (a 60% oil dispersion). The reaction mixture was stirred for 24 h at 130 °C. Then the mixture was allowed to stir to room temperature for 30 min, and 20 mL of ether was added. The organic phase was separated and washed with water three times, dried, filtered, and the solvent was removed by rotary evaporation. The residue was then purified by silica gel column chromatography by elution with 8:2 hexane/ethyl acetate mixtures to yield the title compound **28** (233 mg, 0.795 mmol) in 50% yield as a white solid. Mp: 122−123 °C (hexane/ethyl acetate). IR (KBr), ν (cm^{-1}): 1504 (C═C); 1216 (Ar−O); 1088 (C−O). ^{1}H NMR ($CDCl_3$, 200 MHz) δ (ppm): 2.5 (s, 3H, CH_3−S); 5.73 (m, 1H, C-3H); 6.06 (s, 1H, C-4H); 6.31 (t, 1H, J = 3.8 Hz, C-2H); 7.06 (m, 3H, Ar); 7.21 (dd, J_1 = 3 Hz, J_2 = 1.5 Hz, 1H, C-1H); 7.27 (d, J = 8.4 Hz, 2H, Ar); 7.40 (m, 3H, Ar). ^{13}C NMR ($CDCl_3$, 50.3 MHz) δ (ppm) (∗ indicates interchangeable): 15.7 (CH_3, CH_3−S); 76.0 (CH, C-4); 106.3 (CH, C-3); 110.5 (CH, C-2); 114.7 (CH, C-1); 114.9 (CH, C-9); 118.3 (CH, C-6); 122.3* (CH, C-7); 124.9* (CH, C-8); 126.2 (CH, C-2′, and C-6′); 126.6 (C, C-3a); 127.3 (C, C-1′); 128.5 (CH, C-3′, and C-5′); 134.5 (C, C-9a); 139.4 (C, C-4′); 145.9 (C, C-5a).

4-(*p*-Methylsulfonylphenyl)-4*H*-pyrrolo[2,1-*c*][1,4]benzoxazine (29). 29 was prepared from the corresponding methylthio following the procedure described above. The title compound was obtained as a white solid in 45% yield. Mp: 109−111 °C (hexane/ethyl acetate). IR (KBr), ν (cm^{-1}): 1519 (C═C); 1413 (SO_2); 1224 ((Ar−O); 956 (C−O); 1043 (S═O). ^{1}H NMR ($CDCl_3$, 200 MHz) δ (ppm): 3.10 (s, 3H, CH_3-S); 5.75 (dt, J_1 = 3 Hz, J_2 = 1 Hz, 1H, C-3H); 6.21 (s, 1H, C-4H); 6.33 (t, J = 3 Hz, 1H, C-2H); 7.10 (m, 3H, Ar); 7.23 (dd, J_1 = 3 Hz, J_2 = 1 Hz, 1H, C-1H); 7.40 (m, 1H, C-9H); 7.70 (d, J = 8.2 Hz, 2H, C-2′H, and C-6′H); 7.98 (d, J = 8,2 Hz, 2H, C-3′H, and C-5′H). ^{13}C NMR ($CDCl_3$, 50.3 MHz) δ (ppm) (∗ indicates interchangeable): 44.5 (CH_3, CH_3-); 75.2 (CH, C-4); 106.8 (CH, C-3); 110.7 (CH, C-2); 114.8 (CH, C-1); 115.4 (CH, C-6); 118.3 (CH, C-9); 122.8* (CH, C-7); 125.2* (CH, C-8); 125.8 (C, C-3a); 126.5 (C, C-1′); 127.6 (CH, C-2′, and C-6′); 128.5 (CH, C-3′, and C-5′); 140.6 (C, C-9a); 146.1 (C, C-4′); 145.2 (C, C-5a). Anal Calcd for $C_{18}H_{15}NO_3S$: C, 66.44%; H, 4.65%; N, 4.30%. Found: C, 66.59%; H, 4.77%; N, 4.56%.

Preparation of *N*-Arylanilines 30−33. The preparation of arylanilines **30**−**33** was described previously by us.[21]

(B) Anti-Inflammatory Activity. In Vitro Assay. The ability of the test compound to inhibit the conversion of arachidonic acid to prostaglandin H_2 (PGH_2) was determined using a COX-1/COX-2 inhibitor screening assay kit (catalog no. 560101; Cayman Chemical, Ann Arbor, MI).

Briefly, cyclooxygenase catalyzes the first step in the biosynthesis of arachidonic acid to PGH_2. The COX (ovine) inhibitor screening assay directly measures $PGF_{2\alpha}$ produced by $SnCl_2$ reduction, by enzyme immunoassay (ACE competitive EIA). This assay is based on the competition between PGs and PG−acetylcholinesterase (AChE) conjugate (PG tracer) for a limited amount of PG monoclonal antibody. Because the concentration of PGs varies, the amount of PG tracer that is able to bind to the PGs monoclonal antibody will be inversely proportional to the concentration of PG in the well. This antibody−PG complex binds to goat polyclonal anti-mouse IgG that has been previously attached to the well. The plate was washed to remove any unbound reagents, and Ellman's reagent (which contains the substrate to acetylcholinesterase) is added to the well. The product of this enzymatic reaction absorbs at 405 nm. The intensity of this color, determined spectrophotometrically, is proportional to the amount of PG trace bound to the well, which is inversely proportional to the amount of free PG present in the well during the incubation: absorbance ∝ [bound PG tracer] ∝ 1/[PG].

In Vivo Test. The carrageenin-induced rat paw edema assay was carried out using a modified Winter's method as a preliminary screening test. The rats (in groups of six animals weighing 160−200 g, young adult male Sprague−Dawley) were starved for 24 h before the test compound (70 mg/kg po) was administered. The drugs were given orally 1 h before carrageenan. Rat paw edema was induced by subplantar injection of 0.1 mL of a 1% solution of carrageenan in sterile pyrogen-free 0.9% NaCl solution, and the volume of paw was measured by water displacement in a plethysmometer S-5128, Ugo Basile. Three and four hours after the injection of carrageenan, the volume of the paw was again measured. All statistical analyses of data were processed by computer. Any treatment mean value significantly less than the control mean was indicative of significant anti-inflammatory activity. Rat paw edema volume of treated animals was compared to that animals receiving ibuprofen for comparing the relative potency. No toxic symptoms were observed after oral administration of 70 mg/kg in the animal test.

Antitumor Activity. Cell Lines and Cell Cultures.[24−27] A human chronic myelougenous leukemia cell line, K562, was maintained as suspension cultures in RPMI1640 medium (SIGMA-Aldrich, catalog no. R8758) supplemented with 10% fetal bovine serum (FBS; Sigma-Aldrich, catalog no. F6178), 100 U/mL penicillin/100 μg/mL streptomycin (Sigma-Aldrich, catalog no. P4333), and 0.25 μg/mL amphothericin B (Sigma-Aldrich, catalog no. A2411) at 37 °C in 5% CO_2 (complete medium).

A human nonsmall lung cancer cell line, NCI-H460, a human colon cancer cell line, HT-29, which constitutively expresses COX-2, and a human fibroblastic cell line, HuDe, were cultured in MEM medium (Sigma-Aldrich, catalog no. M4655) supplemented with 10% FBS, 100 U/mL penicillin, 100 μg/mL streptomycin, and 0.25 μg/mL amphothericin B at 37 °C in 5% CO_2.

Proliferation Assay. K562 cell line was cultured in a 24-well microplate by adding 1 mL of complete medium containing 2.0×10^5 cells in the absence or presence of test compounds [10 μM].

The effects of test compounds on cell viability were assayed on a portion of the cell suspension. The cell number was determined with a hemocytometer, and viability was estimated by trypan blue dye exclusion.

Instead, the 3-(4,5-dimethylthiazol-2-yl)-2,5-diphenyltetrazolium bromide (MTT) assay was used to determine cell viability of NCI-H460, HT-29, and HuDe cell lines.

MTT is a yellow tetrazolium salt that is taken up and cleaved only by metabolically active cells, which reduce it to a colored, water-insoluble formazan salt. The solubilized formazan product can be quantified via absorbance at 570 nm (690 nm for blank), which is measured using a 96-well-format spectrophotometer (ELx-800-BioTek instruments). The absorbance correlates directly with the cell number.

Cells were plated at 2.0×10^4 cell/well in 100 μL volume in 96-well plates and grown for 72 h in MEM complete medium. Different concentrations of test drugs or 0.1% DMSO were added to the wells. Then cells were incubated with 10 μL of MTT (5 mg/mL) at 37 °C for 3 h. The tetrazolium crystals were solubilized by the addition of 4.5 mL of isopropyl alcohol−0.5 mL of Triton X-100 in 150 μL of 37% HCl.

Conformational Analysis. Molecular modeling of NSAIDs was carried out on an O2 Silicon Graphics computer using the X-ray crystallography data in the Cambridge Structural Database and conformational analysis The conformational preferences in aqueous solution were determined computations using the geometries optimized at the B3LYP/6-31G(d) level using the program Gaussian 03[28] and the relative free energies of hydration from the MST B3LYP/6-31G(d) version of the PCM continuum model.[29] A systematic exploration at the B3LYP/6-31G(d) level was performed by changing the torsional angle around the bonds CO−Ar and C−N−R^1−R^2 by increments of 60° and excluding those conformers where a steric clash was observed. The geometry of the local minimum energy structures was then fully optimized. The minimum energy nature of all the stationary points located from B3LYP/6-31G(d) geometry optimizations was verified from the analysis of the vibrational frequencies, which were positive in all cases.

For all compounds the MO (molecular orbitals) wave functions were determined and the following properties were examined: energies of the HOMO, NHOMO, LUMO, and NLUMO frontier orbitals, net atomic charges, dipole moment (MD), and the free energy of solvatation (ΔGsolv).

The energy of the HOMO is related to the ionization potential and characterizes the molecular reactivity in front of the attack by electrophiles, while the energy of the LUMO is related to the electron affinity and describes the reactivity toward nucleophiles. In processes involving radicalary species, both HOMO and LUMO have a large contribution. The HOMO−LUMO gap, i.e., the difference in energy between the HOMO and the LUMO, is an important stability index. A large HOMO−LUMO gap implies high stability for the molecule because of its lower reactivity in chemical reactions. The HOMO−LUMO gap has thus been used as an approximation to the excitation energy of the molecule.

Overall, there are two major conformational families that differ in the relative orientation of the aromatic rings and several subfamilies that arise from rotation about the R_1SO_2 bond. The energy differences among them were sufficiently small to consider them all as candidates for the bound conformation; other conformers were located, but they were not considered because of the large destabilization (more than 4 kcal/mol) relative to the most stable conformer.

Molecular Modeling Methods. NSAID docking was done in mouse COX-2 enzyme taken from X-ray crystallographic structures, complexed to flubiprofen (3PGH),[30] diclofenac (1PXX),[31] and SC-558 (6COX).[32] The X-ray crystal structure of COX-2 with an inhibitor SC-558 was treated as a template molecule to construct the complexes of COX-2 with NSAIDS.

The AutoDock 3.0 program[33] was used to explore the docking for different conformations of the 15 NSAIDs in the active site of the enzyme. The AutoDock exploration was carried out within a 30 Å cube by using 0.25 Å grid spacing. Seven affinity grids were calculated (C, N, O, S, H, Cl, F).

The simulated annealing protocol consisted of 100 runs of 50 cycles, each cycle including 25 000 accepted or 25 000 rejected relative positions. A distance dependent dielectric constant equal to 4r was used to simulate a partially solvated state. The annealing temperature was set to 298 K during the first cycle and then linearly reduced at the end of each cycle.

Ligands were considered conformationally flexible by defining the torsion angles about which rotation was allowed. AutoDock 3.0 was used to generate conformer binding mode with the lowest docked energy. From the 100 simulations with each compound, the COX-2−ligand complex structures in the top ranked energy cluster were selected. To take into account protein flexibility, the stability and behavior of all complexes were studied in a dynamic context and the van der Waals and electrostatic components of the interaction energy monitored. Further analysis of the binding orientation of the aryl methyl sulfones indicated that this substituent adopts the arylpropionic position of flurbiprofen in the crystal structure of COX-2 (3PGH).[30]

The lowest docked energy resulting complexes were energy-minimized and equilibrated using the AMBER 10 program.[34] The standard ionization state at neutral pH was considered for the ionizable residues. The system was hydrated by an octahedral box of TIP3P water molecules extending 11 Å outside the protein at all sides, resulting in an average of 13 850 waters. The parm-99 file of the AMBER force field was used to describe the enzyme. Restricted electrostatic potential fitted charges determined at the HF/6-31G(d) level, using the RESP procedure and van der Waals parameters taken for related atom types in the AMBER-99 force field, were used for each inhibitor. Torsional parameters for the methylsulfone group were taken from those reported in our previous studies.[35−38] SHAKE was used to maintain all the bonds at their equilibrium distances, and a nonbonded 11 Å cutoff and a distance-dependent dielectric constant were used throughout. In each case, 100 steps of steepest descent were followed by conjugate gradient until the root-mean-square value of the potential energy gradient was below 0.01 kcal mol^{-1} A^{-1}.

The system was equilibrated by running five 60 ps molecular dynamics (MD) simulations to increase the temperature to 298 K. Subsequently a 10 ns MD simulation was carried out with an integration time step of 2 fs.

In all cases the positional root-mean square deviations (rmsd) determined for the backbone and heavy atoms in the system with regard to the corresponding X-ray crystallographic structure was in the range 0.9−1.8 Å. The characterization of the structural features that mediate the binding to the enzyme was determined by averaging the geometrical parameters for the snapshots (saved every ps) sampled along the last 2 ns of the MD simulation. The ptraj module of AMBER was used to perform most numerical analyses of the MD trajectories.

To refine the structures to be used for free energy analysis, energy minimizations of the entire protein−ligand complexes were performed in implicit water solvent models.

The solvated complexes were minimized with 2000 steps of conjugate-gradient minimization without restraints, employing a residue-based cutoff of 11 Å. After each energy minimization, visual inspection of the complexes was performed to make sure that the protein and the ligand remained close to conformation observed in the crystal structures.

MM-GBSA Computations. The calculation and decomposition of binding free energy, ΔG_{bind}(MM-GBSA), between protein and ligands were evaluated using the MM-GBSA (molecular

mechanics generalized Born/surface area) method as implemented in AMBER 9.[37]

MM-GBSA has consistently been shown to be a good method for comparing binding energies of complexes similar to those in this case.[38,39] MM-GBSA computes the binding free energy by using a thermodynamic path that combines the molecular mechanical energies with the continuum solvent approaches.

In the MM-GBSA method, the total binding free energy in water is approximated by $\Delta G_{bind} = \Delta E_{GAS} + \Delta G_{GB} + \Delta G_{SUR}$. The ΔE_{GAS} is the energy difference of the solutes in the two (bound and unbound) states. The ΔG_{GB} is the polar part of the solvation free energy represented by the generalized Born approach. The ΔG_{SUR} is the apolar surface part of the free energy solvation of a cavity inside the solvent). In this formula, the conformational entropy of the solute is not explicitly considered, although the solvent entropy is implicitly considered in the ΔG_{GB} and ΔE_{GAS}.

The electrostatic term is computed by adding the solvent screened electrostatic interaction between ligand and enzyme, and the corresponding change in the desolvation free energy of the ligand upon binding. According to this procedure, the desolvation cost of the enzyme is assumed to be common for all complexes between COX-2 and inhibitors, which is justified by the fact that all of them share a common chemical skeleton and occupy the same position in the binding site while providing a substantial saving in computer time.

MM-GBSA computations were performed for a set of 100 structures of the enzyme−inhibitor complex taken from the last 2 ns of the MD simulation and were obtained using the Amber package. Prior to the calculations, the complexes were energy-minimized to eliminate bad contacts; at the end all water molecules were removed. The relative binding affinity was determined from the most favorable binding free energies determined for each inhibitor.

Acknowledgment. The authors express their sincere gratitude to the Ministerio de Ciencia y Tecnología (Grant CTQ2007-60614/BQU) and the Departament d'Universitats, Recerca i Societat de la Informació de la Generalitat de Catalunya, Spain (Grant 2005-SGR-00180), for the financial support. J.B. acknowledges the Generalitat de Catalunya for a predoctoral fellowship.

Supporting Information Available: Dipole moments (Figure 2A−C), molecular modeling studies (Figure 6−8), and the preparation of organic compounds. This material is available free of charge via the Internet at http://pubs.acs.org.

References

(1) (a) Bertolini, A.; Ottani, A.; Sandrini, M. Selective COX-2 inhibitors and dual anti-inflammatory drugs: critical remarks. *Curr. Med. Chem.* **2002**, *9*, 1033–1043. (b) Howardell, M. J., Ed. *COX-2 Inhibitor Research*; Nova Science: New York, 2006. (c) Yu, G.; Praveen Rao, P. N.; Chowdhury, M. A.; Abdellatif, K. R. A.; Dong, Y.; Das, D.; Velázquez, C. A.; Suresh, M. R.; Knaus, E. E. Synthesis and biological evaluation of N-difluoromethyl-1,2-dihydropyrid-2-one acetic acid regioisomers: dual inhibitors of cyclooxygenases and 5-lipoxygenase. *Bioorg. Med. Chem. Lett.* **2010**, *20*, 2168–2173. (d) Chowdhury, M. A.; Abdellatif, K. R. A.; Dong, Y.; Das, D.; Suresh, M. R.; Knaus, E. E. Synthesis of celecoxib analogues possessing a N-difluoromethyl-1,2-dihydropyrid-2-one 5-lipoxygenase pharmacophore: biological evaluation as dual inhibitors of cyclooxygenases and 5-lipoxygenase with anti-inflammatory activity. *J. Med. Chem.* **2009**, *52*, 1525–1529.

(2) (a) Dannhardt, G.; Kiefer, W. Cyclooxygenase inhibitors—current status and future prospects. *Eur. J. Med. Chem.* **2001**, *36*, 109–126. (b) Puig, C.; Crespo, M. I.; Godessart, N.; Feixas, J.; Ibarzo, J.; Jiménez, J. M.; Soca, L.; Cardelus, I.; Heredia, A.; Miralpeix, M.; Puig, J.; Beleta, J.; M. Huerta, J. M.; López, M.; Segarra, V.; Ryder, H.; Palacios, J. M. Synthesis and biological evaluation of 3,4-diaryloxazolones: a new class of orally active cyclooxygenase-2 inhibitors. *J. Med. Chem.* **2000**, *43*, 214–223. (c) Kiefer, W.; Dannhardt, G. Novel insights and therapeutical applications in the field of inhibitors of COX-2. *Curr. Med. Chem.* **2004**, *11*, 3147–3161.

(3) Gund, P.; Shen, T. Y. A model for the prostaglandin synthetase cyclooxygenase site and its inhibition by antiinflammatory arylacetic acids. *J. Med. Chem.* **1977**, *20*, 1146–1152.

(4) Jouzeau, J. Y.; Terlain, B.; Abid, A.; Nedelec, E.; Netter, P. Cyclooxygenase isoenzymes. How recent findings affect thinking about nonsteroidal anti-inflammatory drugs. *Drugs* **1997**, *53*, 563–582.

(5) (a) Mc Gettigan, P.; Henry, D. Current problems with non-specific COX inhibitors. *Curr. Pharm. Des.* **2000**, *6*, 1693–1724. (b) Barbaric, M.; Kralj, M.; Marjanovic, M.; Husnjak, I.; Pavelic, K.; Filipavic-Grcic, J.; Zorc, D.; Zorc, B. Synthesis and in vitro antitumor effect of diclofenac and fenoprofen thiolated and non-thiolated polyaspartamide-drug conjugates. *Eur. J. Med. Chem.* **2007**, *42*, 20–29.

(6) Moore, B. C.; Simmons, D. L. COX-2 inhibition. Apoptosis and chemoprevention by nonsteroidal anti-inflammatory drugs. *Curr. Med. Chem.* **2000**, *7*, 1131–1144.

(7) Chen, L.; He, Y.; Huang, H.; Liao, H.; Wei, W. Selective COX-2 inhibitor celecoxib combined with EGFR-TKI ZD 1839 on non-small cell lung cancer cell lines: in vitro toxicity and mechanism study. *Med. Oncol.* **2008**, *25*, 161–171.

(8) Thun, M. J.; Henley, S. J.; Pairono, C. Nonsteroidal anti-inflammatory drugs as anticancer agents: mechanistic, pharmacologic, and clinical issues. *J. Natl. Cancer Inst.* **2002**, *94*, 252–266.

(9) Soh, J.-W.; Kazi, J. V.; Li, H.; Thompson, W. J.; Weinstein, B. Celcoxib-induced growth inhibition in SW480 colon cancer cells is associated with activation of protein kinase G. *Mol. Carcinog.* **2008**, *47*, 519–525.

(10) Harris, R. E.; Beebe-Donk, J.; Doss, H.; Burr-Doss, D. Aspirin, ibuprofen, and other non-steroidal anti-inflammatory drugs in cancer prevention: a critical review of non-selective COX-2 blockade (review). *Oncol. Rep.* **2005**, *13*, 559–583.

(11) Arber, N.; Levin, B. Chemoprevention of colorectal neoplasia: the potential for personalized medicine. *Gastroenterology* **2008**, *134*, 1224–1237.

(12) Williams, J. L.; Borgo, S.; Hasan, I.; Castillo, E.; Traganos, F.; Rigas, B. Nitric oxide-releasing nonsteroidal anti-inflammatory drugs (NSAIDs) alter the kinetics of human colon cancer cell lines more effectively than traditional NSAIDs: implications for colon cancer chemoprevention. *Cancer Res.* **2001**, *61*, 3285–3289.

(13) Robak, P.; Smolewski, P.; Robak, T. The role of non-steroidal anti-inflammatory drugs in the risk of development and treatment of hematologic malignances. *Leuk. Lymphoma* **2008**, *49*, 1452–1462.

(14) Chen, L. C.; Ashcroft, D. M. Risk of myocardial infarction associated with selective COX-2 inhibitors: meta-analysis of randomised controlled trials. *Pharmacoepidemiol. Drug Saf.* **2007**, *16*, 762–772.

(15) Peri, K. G.; Hardy, P.; Li, D. Y.; Varma, D. R.; Chemtob, S. Prostaglandin G/H synthase-2 is a major contributor of brain prostaglandins in the newborn. *J. Biol. Chem.* **1995**, *270*, 24615–24620.

(16) Capilla, A. S.; Pujol, M. D. A convenient method for the preparation of substituted naphtho[2,3-*b*]-1,4-dioxin by the Diels−Alder reaction. *Synth. Commun.* **1996**, *26*, 1729–1738.

(17) Vázquez, M. T.; Rosell, G.; Pujol, M. D. Synthesis and anti-inflammatory activity of *rac*-2-(2,3-dihydro-1,4-benzodioxin)propionic acid and its *R* and *S* enantiomers. *Eur. J. Med. Chem.* **1997**, *32*, 529–534 and references cited herein.

(18) Hamdouchi, C.; de Blas, J.; Ezquerra, J. A novel application of the Ullmann coupling reaction for the alkylsulfenylation of 2-aminoimidazo[1,2-*a*]pyridine. *Tetrahedron* **1999**, *55*, 541–552.

(19) Lindley, J. Copper-assisted nucleophilic substitution of aryl halogen. *Tetrahedron* **1984**, *40*, 1433–1438.

(20) Sánchez, I.; Pujol, M. D. A convenient synthesis of pyrrolo[2,1-*c*][1,4]benzodioxines. *Tetrahedron* **1999**, *55*, 5593–5598.

(21) Romero, M.; Harrak, Y.; Basset, J.; Ginet, L.; Constans, P.; Pujol, M. D. Preparation of *N*-arylpiperazines and other *N*-aryl compounds from aryl bromides as scaffolds of bioactive compounds. *Tetrahedron* **2006**, *62*, 9010–9016.

(22) Lozano, J. J.; López, M.; Ruiz, J.; Vázquez, I. J.; Pouplana, R. QSAR in the Nonsteroidal Antiinflammatory Agents: The Fenamic Acids. *Trends in QSAR and Molecular Modelling 92*; Wermuth, C. G., Ed.; ESCOM: Leiden, The Netherlands, 1993; pp 560−61.

(23) Limongelli, V.; Bonomi, M.; Marinelli, L.; Gervasio, F. L.; Cavalli, A.; Novellino, E.; Parrinello, M. Molecular basis of cyclooxygenase enzymes (COXs) selective inhibition. *Proc. Natl. Acad. Sci. U.S.A.* **2010**, *107*, 5411–5416.

(24) Waskewich, C.; Blumenthal, R. D.; Li, H.; Stein, R.; Goldenberg, D. M.; Burton, J. Celecoxib exhibits the greatest potency amongst cyclooxigenase (COX) inhibitors for growth inhibition of COX-2 negative hemapoietic and epithelial cell lines. *Cancer Res.* **2002**, *62*, 2029–2033.

(25) Giles, J. F.; Kantarjian, H. M.; Bekele, B. N.; Cortes, J. E.; Faderl, S.; Thomas, D. T.; Manshouri, T.; Rogers, A.; Keating, M. J.;

Talpaz, M.; O'Brien, S.; Albitar, M. Bone marrow cyclooxygenase-2 levels are elevated in chronic phase chronic myeloid leukaemia and are associated with reduced survival. *Br. J. Haematol.* **2002**, *119*, 38–45.

(26) Cianchi, F.; Cortesini, C.; Fantappie, O.; Messerini, L.; Sardi, I.; Lasagna, N.; Perna, F.; Fabbroni, V.; Di Felice, A.; Perigli, G.; Mazzanti, R.; Masini, E. Cyclooxygenase-2 activation mediates the proangiogenic effect of nitric oxide in colorectal cancer. *Clin. Cancer Res.* **2004**, *10*, 2694–2704.

(27) Shin, Y. K.; Park, J. S.; Kim, H. S.; Jun, H. J.; Kim, G. E.; Suh, C. O.; Yun, Y. S.; Pyo, H. Radiosensivity enhancement by celecoxib, a cyclooxygenase (COX)-2 selective inhibitor, via COX-2-dependent cell cycle regulation on human cancer cells expressing differential COX-2 levels. *Cancer. Res.* **2005**, *65*, 9501–9509.

(28) Frisch, M. J.; Trucks, G. W.; Schlegel, H. B.; Scuseria, G. E.; Robb, M. A.; Cheeseman, J. R.; Montgomery, J. A., Jr.; Vreven, T.; Kudin, K. N.; Burant, J. C.; Millam, J. M.; Iyengar, S. S.; Tomasi, T.; Barone, V.; Mennucci, B.; Cossi, M.; Scalmani, G.; Rega, N.; Petersson, G. A.; Nakatsuji, H.; Hada, M.; Ehara, M.; Toyota, K.; Fukuda, R.; Hasegawa, J.; Ishida, M.; Nakajima, T.; Honda, Y.; Kitao, O.; Nakai, H.; Klene, M.; Li, X.; Knox, J. E.; Hratchian, H. P.; Cross, J. B.; Bakken, V.; Adamo, C.; Jaramillo, J.; Gomperts, R.; Stratmann, R. E.; Yazyev, O.; Austin, A. J.; Cammi, R.; Pomelli, C.; Ochterski, J. W.; Ayala, P. Y.; Morokuma, K.; Voth, G. A.; Salvador, P.; Dannenberg, J. J.; Zakrzewski, V. G.; Dapprich, S.; Daniels, A. D.; Strain, M. C.; Farkas, O.; Malick, D. K.; Rabuck, A. D.; Raghavachari, K.; Foresman, J. B.; Ortiz, J. B.; Cui, Q.; Baboul, A. J.; Clifford, S.; Cioslowski, J.; Stefanov, B. B.; Liu, G.; Liashenko, A.; Piskorz, P.; Komaromi, I.; Martin, R. L.; Fox, D. J.; Keith, T.; Al-Laham, M. A.; Peng, C. Y.; Nanayakkara, A.; Challacombe, M.; Gill, P. M. W.; Johnson, B.; Chen, W.; Wong, M. W.; Gonzalez, C.; Pople, J. A.. *Gaussian 03*, revision D.02; Gaussian, Inc.: Wallingford, CT, 2004.

(29) Soteras, I.; Curuchet, A.; Bidon-Chanal, A.; Orozco, M.; Luque, F. J. Extensión of the MST model to the IEF formalism: HF and B3LYP parametrizations. *J. Mol. Struct.: THEOCHEM* **2005**, *727*, 29–40.

(30) Kurumbail, R. G; Stevens, A. M; Gierse, J. K.; McDonald, J. J.; Stegeman, R. A.; Pak, J. Y.; Gildehaus, D.; Miyashiro, J. M.; Penning, T. D.; Seibert, K; Isakson, P. C.; Stallings, W. C. Structural basis for selective inhibition of cyclooxygenase-2 by anti-inflammatory agents. *Nature* **1996**, *384*, 644.

(31) Rowlinson, S. W.; Kiefer, J. R.; Prusakiewicz, J. J.; Pawliotz, J. L.; Kozak, K. R.; Kalgutkar, A. S.; Stallings, W. C.; Kurumbail, R. G.; Marnett, L. J. A novel mechanism of cyclooxygenase-2 inhibition involving interactions with Ser-530 and Tyr-385. *J. Biol. Chem.* **2003**, *278*, 45763.

(32) Kurumbail, R. G.; Stevens, A. M; Gierse, J. K.; McDonald, J. J.; Stegeman, R. A.; Pak, J. Y.; Gildehaus, D.; Miyashiro, J. M.; Penning, T. D.; Seibert, K; Isakson, P. C.; Stallings, W. C. Structural basis for selective inhibition of cyclooxygenase-2 by anti-inflammatory agents. *Nature* **1997**, *385*, 555.

(33) Morris, G. M.; Goodsell, D. S.; Halliday, R. S.; Huey, R.; Hart, W. E.; Belew, R. K.; Olson, A. J. Automated docking using a Lamarckian genetic algorithm and empirical binding free energy function. *J. Comput. Chem.* **1998**, *19*, 1639–1662.

(34) Case, D. A.; Darden, T. A.; Cheatham, T. E.; Simmerling, C. L.; Wang, J.; Duke, R. E.; Luo, R.; Crowley, M.; Walker, R. C.; Zhang, W.; Merz, K. M.; Wang, B.; Hayik, S.; Roitberg, A.; Seabra, G.; Kolossváry, I.; Wong, K. F.; Paesani, F.; Vanicek, J.; Wu, X.; Brozell, S. R.; Steinbrecher, T.; Gohlke, H.; Yang, L.; Tan, C.; Mongan, J.; Hornak, V.; Cui, G.; Mathews, D. H.; Seetin, M. G.; Sagui, C.; Babin, V. Kollman, P. A. *AMBER 10*; University of California: San Francisco, CA, 2008.

(35) Pouplana, R.; Lozano, J. J.; Pérez, C; Ruiz, J. Structure-based QSAR study on differential inhibition of human prostaglandin endoperoxide H synthase-2 (COX-2) by nonsteroidal anti-inflammatory drugs. *J. Comput.-Aided Mol. Des.* **2002**, *16*, 683–710.

(36) Pouplana, R.; Lozano, J. J.; Ruiz, J. Molecular modeling of the differential interaction between several non-steroidal anti-inflammatory drugs and human prostaglandin endoperoxide H synthase-2 (H-PGHS-2). *J. Mol. Graphics Modell.* **2002**, *20*, 329–343.

(37) Kollman, P. A.; Massova, I; Reyes, C. Calculating structures and free energies of complex molecules: combining molecular mechanics and continuum models. *Acc. Chem. Res.* **2000**, *33*, 889–897.

(38) Srinivasan, J.; Cheatham, T. E.; Cieplak, P.; Kollman, P. A.; Case, D. A. Continuum solvent studies of the stability of DNA, RNA, and phosphoramidate-DNA helices. *J. Am. Chem. Soc.* **1998**, *120*, 9401–9409.

(39) Pérez, C.; Sánchez, J.; Mármol, F.; Puig-Parellada, P.; Pouplana, R. Reactivity of biologically important NSAID compounds with superoxide ($O2\cdot-$) and nitric oxide ($\cdot NO$) and cyclooxygenase inhibition. *QSAR Comb. Sci.* **2007**, *26*, 368–377.